

Potential photoacid generators based on oxime sulfonates

Journal of Chemical Research
2019, Vol. 43(1-2) 26–33
© The Author(s) 2019
Article reuse guidelines:
sagepub.com/journals-permissions
DOI: 10.1177/1747519819831829
journals.sagepub.com/home/chl



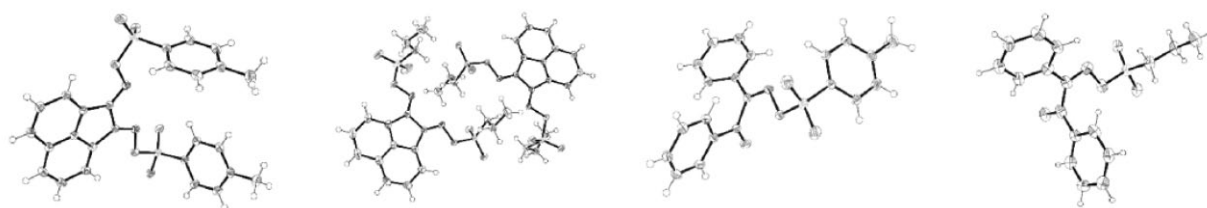
M John Plater, William TA Harrison and Ross Killah

Abstract

The bis-oxime of acenaphthenequinone and the mono-oxime of benzil have been sulfonated by reaction with 4-methylbenzenesulfonyl chloride and propylsulfonyl chloride. The four sulfonated oximes were characterised by X-ray single-crystal structure determinations. Some photochemical decompositions were studied using a 6-W 254-nm immersion well lamp in dichloromethane. The 4-methylbenzenesulfonate bis-oxime of acenaphthenequinone and the 4-methylbenzenesulfonate mono-oxime of benzil both give 4-methylbenzenesulfonic acid upon irradiation but not 4-methylbenzenesulfinic acid. Fragmentation pathways are discussed. The possible use of these compounds as photoacid generators in polymer resists and the role of secondary reactions to liberate acid is discussed.

Keywords

acenaphthenequinone, benzil, oxime sulfonates, photoacid generator



Introduction

Improvements in the performance of semiconductor devices arise because of the decreasing size of the features on a silicon chip.¹ Gordon E Moore,² a co-founder of Intel, made the observation in 1965 that circuit densities of semiconductors would continue to double on a regular basis. This has become known as Moore's Law and illustrates the astounding developments made in the field (Figure 1).¹

Semiconductor devices or computer chips are fabricated by microlithography (Figure 2).¹ In this technology, a radiation-sensitive polymer is spin coated and dried, forming a thin film of 1–0.1 μm thickness, on a single-crystal silicon wafer forming a resist. This is irradiated through a mask forming a pattern and then the exposed resist films are developed to create images. If the irradiated image is more soluble, it is classed as a positive system, and if it is less soluble, it is classed as a negative system. The remaining resist film serves as a protective layer during etching of the substrate. After etching, the remaining resist film is removed leaving behind a circuit pattern. The process is repeated to fabricate complex semiconductor devices.

The resists contain a light-sensitive compound which upon irradiation and development modifies the solubility properties of the resist polymer (Figure 3).^{3,4} The success of

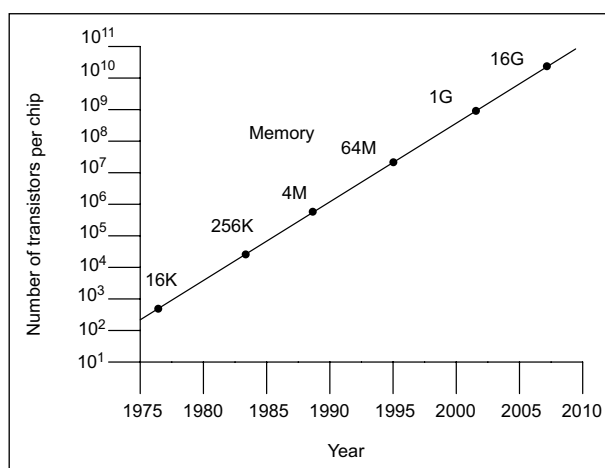


Figure 1. A chart illustrating Moore's Law.

Department of Chemistry, University of Aberdeen, Aberdeen, UK

Corresponding author:

M John Plater, Department of Chemistry, University of Aberdeen,
Meston Walk, Aberdeen AB24 3UE, UK.
Email: m.j.plater@abdn.ac.uk

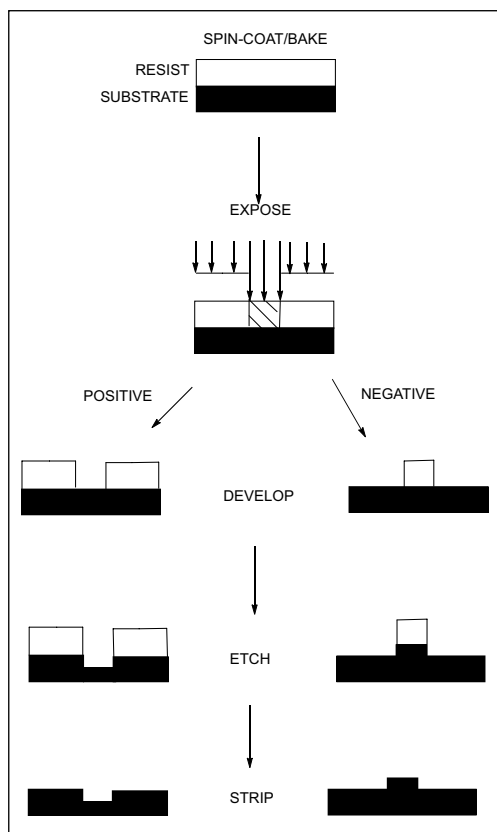


Figure 2. The lithographic imaging process.

the semiconductor industry's recent developments has been due to the use of photoacid generators (PAGs) which liberate a small quantity of acid that *catalyses* a chemical reaction in a development step. For example, acid-catalysed deprotection of *tert*-butyl esters, liberating isobutene, leaves polymer-bound carboxylic acids which solubilise the polymer in aqueous base. Compounds **1** and **2** are likely to liberate the acid of a stable counter-anion,^{5–7} whereas compounds **3–5** will liberate a sulfonic acid.^{3,4,8–11} Decreasing feature size is commensurate with the use of higher energy radiation ranging from the ultraviolet (UV; 450–190 nm) down to extreme ultraviolet (EUV) at 7 nm.^{3,12–14}

Figure 4 shows a possible mechanism for the photochemical fragmentation of a Crivello or triarylsulfonium salt.³ The non-nucleophilic counter-ion becomes the anion of a strong acid HX. A ring proton of the Crivello salt **1** is substituted for the phenyl ring and becomes the proton of the strong acid.

The aim of this project is to develop an understanding of how the class of photoacid generators based on sulfonated oximes can function to modify polymer resists. Some compounds that are representative of examples in the literature^{4,8,10,11} have been prepared and their photochemical decomposition products studied.

Results and discussion

The condensation of NH_2OH with acenaphthenequinone gives the known bis-oxime **9**¹⁵ and with benzil gives the known mono-oxime **10**¹⁶ only and not a bis-oxime of benzil

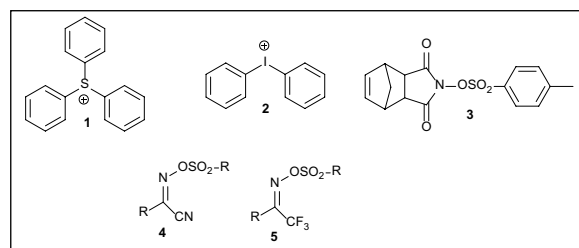


Figure 3. Some representative photoacid generators where R = different alkyl and aryl groups.

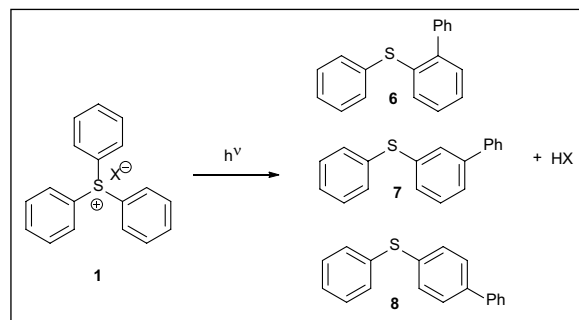


Figure 4. The photochemical fragmentation of a triphenylsulfonium salt to give a phenylthio-substituted biaryl and a strong acid.

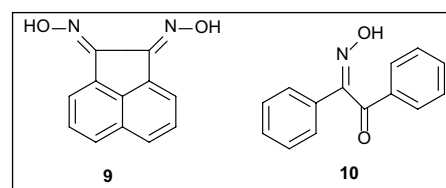


Figure 5. Oximes of acenaphthenequinone **9** and benzil **10**.

which is sometimes reported (Figure 5). There are a number of erroneous literature reports claiming that the bis-oxime of benzil can be formed under these conditions.^{17–19} Both *syn* and *anti* isomers of benzil derivative **10** have been claimed as they can be separated and the *anti* isomers form metal-ion complexes.¹⁶ We found that compounds **9** and **10** were both sulfonated with either 4-methylbenzenesulfonyl chloride or propylsulfonyl chloride to give compounds **11–14** which are potential photoacid generators (Figure 6). They have been characterised by X-ray single-crystal structure determination. The crystal structures show the stereochemistry of these compounds and that of the oximes from which they were made. Only one isomer was formed for each compound **11–14**. Compounds **11** and **12** have both the sulfonate groups pointing away from each other which will arise for steric reasons. However, compounds **13** and **14** are *syn* isomers and are stable. According to the literature, the *anti* isomer **15** is unstable during synthesis for stereoelectronic reasons.¹⁶ It is made from the photochemically isolated *anti* oxime.¹⁶ The molecule fragments with the N-OSO₂R group *trans* to the C–CO bond. In contrast to this, the stability of the *syn* isomers **13** and **14** is striking. The mono-oxime of benzil **10** initially forms as an oil but

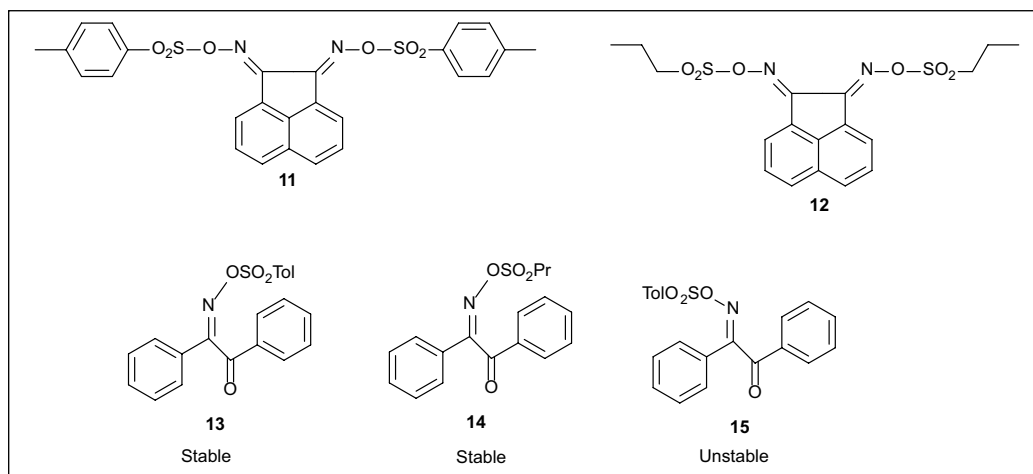


Figure 6. Oxime sulfonates **11–14** characterised by single-crystal X-ray structure determinations and a proposed unstable sulfonate **15**.¹⁶ (Tol = 4-MeC₆H₄-, Pr = propyl-).

Table 1. Comparison of key crystallographic data for oxime sulfonates **11–14**.

Compound	C–N (Å)	N–O (Å)	C–N–O (°)	N–O–S (°)	C–N–O–S (°)
11 S1 branch	1.2817 (19)	1.4449 (15)	107.20 (11)	111.48 (8)	–176.27 (10)
11 S2 branch	1.2844 (18)	1.4372 (15)	107.88 (11)	111.98 (8)	174.10 (9)
12 S1 branch	1.2828 (18)	1.4380 (14)	108.64 (11)	109.65 (8)	–169.20 (9)
12 S2 branch	1.2846 (17)	1.4427 (13)	108.26 (10)	110.13 (7)	169.22 (9)
12 S3 branch	1.2840 (17)	1.4347 (13)	108.96 (10)	110.23 (7)	–175.69 (8)
12 S4 branch	1.2839 (17)	1.4399 (13)	107.89 (10)	110.99 (7)	–165.68 (9)
13	1.282 (3)	1.459 (2)	108.25 (17)	109.28 (12)	–165.15 (14)
14	1.288 (9)	1.463 (7)	107.3 (6)	110.9 (4)	179.6 (4)
FABWAI ²⁰	1.281	1.438	109.3	110.3	–176.5
IBUNOI ²¹	1.269	1.410	110.0	111.3	175.5
IQOQAG ²²	1.274	1.422	110.2	109.9	–177.4
KEBSIW ²³	1.273	1.415	111.6	109.8	–179.3
KEBSOC ²³	1.269	1.438	111.6	111.1	169.6

FABWAI: *N,N*-bis((methylsulfonyl)oxy)-1,2-diphenylethane-1,2-diimine; IBUNOI: (1-(4-bromo-3-(methylsulfonyl)thien-2-yl)-2,2,2-trifluoroethaneiminoyl)-*N*-methylsulfonate; IQOQAG: (2,2-dimethyl-6-((trityloxy)methyl)tetrahydrofuro(3,4-*d*)(1,3)dioxol-4-yl)((methylsulfonyl)oxy)imino)acetonitrile; KEBSIW: 1-[[[(methylsulfonyl)oxy]imino] (4-nitrophenyl)methyl]pyridin-1-ium trifluoromethanesulfonate; KEBSOC: 1-[[*N*-[(methylsulfonyl)oxy]ethanimidoyl]pyridin-1-ium trifluoromethanesulfonate.

slowly crystallises to a white solid after a few hours and is a single isomer by ¹H and ¹³C nuclear magnetic resonance (NMR).

X-ray single-crystal structures

Key geometrical data for **11–14** and known oxime sulfonate crystal structures are compiled in Table 1.

It may be seen that the C=N and N–O distances of the oxime groups in **11–14** and in other known oxime sulfonate crystal structures^{20–23} are all very consistent, as are the C=N–O and N–O–S bond angles. The C=N–O–S torsion angles indicate a preference for near planarity for these atoms, which is assumed to be the most stable conformation for oximes²⁴ and any small deviations might be ascribed to packing forces in the crystal.

In compound **11** (Figure 7), the dihedral angles between the C1–C12 ring system and the pendant C13–C18 and C20–C25 phenyl groups are 81.49 (6)° and 66.93 (6)°, respectively. In the crystal of compound **11**, the molecules are linked by weak C–H⋯O interactions.

Compound **12** crystallises with two molecules in the asymmetric unit (Figure 8) with very similar geometries apart from the propyl chains of the sulfonate groups. In the S1 molecule, both of these adopt *anti* conformations [S1–C13–C14–C15 = –178.27(13)°; C2–C16–C17–C18 = 171.17 (10)°], whereas in the S3 molecule one is *gauche* and one is *anti* [S3–C31–C32–C33 = –60.66 (15)°; S4–C34–C35–C36 = –171.53 (11)°]. In the crystal of compound **12**, the molecules are linked by weak C–H⋯O and C–H⋯N interactions.

In compound **13** (Figure 9), the dihedral angles involving the C10–C16 ring (A), the C16–C21 ring (B) and the C1–C6 ring (C) are *A/B* = 87.28 (11)°, *A/C* = 50.74 (11)° and *B/C* = 44.88 (11)°. The N1–C8–C9=O4 torsion angle is –94.6 (2)°. In the crystal of compound **13**, the molecules are linked by weak C–H⋯O interactions.

In compound **14** (Figure 10), the dihedral angle between the C1–C6 and C9–C14 benzene rings is 77.3 (2)° and the propyl chain adopts an extended conformation [S1–C15–C16–C17 = 176.1 (6)°]. In the crystal of compound **14**, the molecules are linked by weak C–H⋯O interactions.

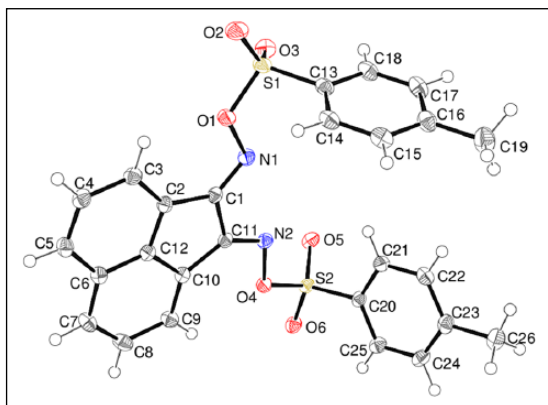


Figure 7. The molecular structure of compound **11** showing 50% displacement ellipsoids.

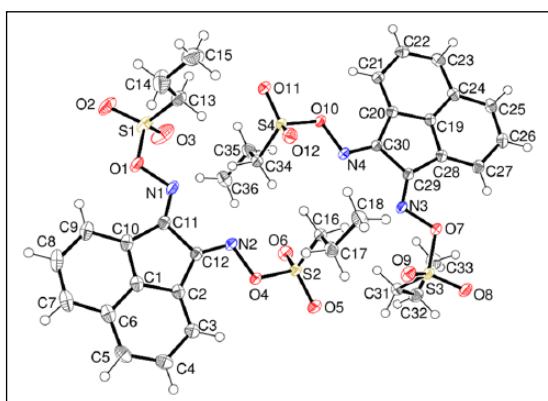


Figure 8. The molecular structure of compound **12** showing 50% displacement ellipsoids.

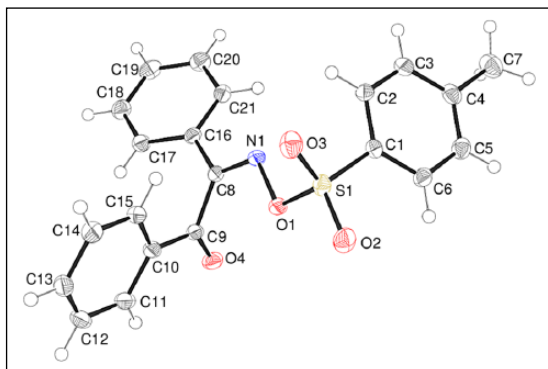


Figure 9. The molecular structure of compound **13** showing 50% displacement ellipsoids.

Photochemical irradiation

Compounds **11** and **13**, representative of many other compounds,^{4,8,10,11} were irradiated in CH_2Cl_2 with a 6-W 254-nm lamp in a 100-mL immersion well for 5 h. This was done without deoxygenation because some polymer resist films are irradiated in air (365 nm i line, 248 nm KrF laser and 193 nm ArF laser by a dry process). Thin-layer chromatography (TLC) analysis of the mixture after evaporation of the solvent showed that the starting material had been consumed. Figure 11 shows some of the possible fragmentation products **16–19**. These might form by a light-catalysed fragmentation of the oxime N–O bond

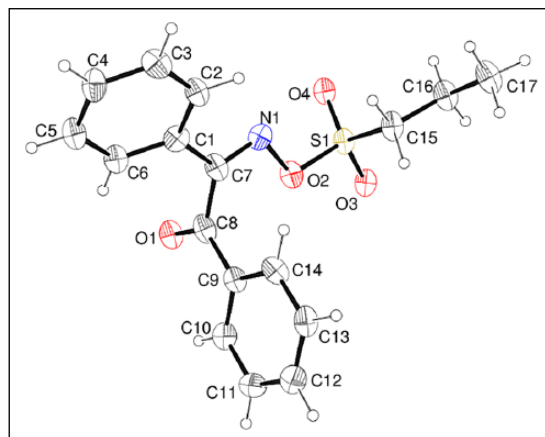


Figure 10. The molecular structure of compound **14** showing 30% displacement ellipsoids.

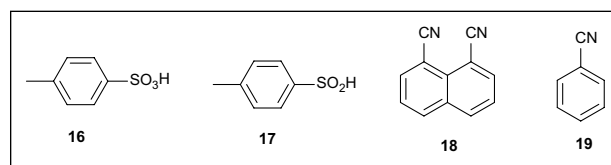


Figure 11. Some possible products from the photochemical decomposition of compounds **11** and **13**.

followed by a secondary reaction of the sulfonate radical such as hydrogen abstraction from the solvent (Figure 12). Termination of free radicals after irradiation could also occur by recombination which could give peroxide **22**. This peroxide **22** would require heating, in a development step, or hydrolysis to release acid **16**. In these studies, only evidence for 4-methylbenzenesulfonic acid **16** has been found. ^1H NMR analysis of the crude product in D_2O , from the irradiation of compounds **11** and **13**, showed two strong aromatic doublets and an upfield singlet which matched the spectrum for the standard 4-methylbenzenesulfonic acid **16**. This assignment was confirmed by comparison of the ^{13}C NMR data with standards of 4-methylbenzenesulfonic acid **16** and 4-methylbenzenesulfinic acid **17**. Again, the data matched those for the standard **16** including the chemical shift at 142.3 ppm of the quaternary carbon attached to the sulfur atom. This occurs at a different chemical shift of 150.5 ppm for the sulfinic acid **17**. Compound **13** released acid more efficiently than compound **11** as the ^1H NMR data were stronger and cleaner. It was difficult to identify other products from the crude mixtures. However, no nitriles such as compound **18** or **19**, which might form from radical **20**, were detected by ^1H NMR in CD_3OD or by the benzonitrile infrared (IR) stretch at 2228 cm^{-1} . The fate of species **20** is unknown. A water extract of both products turned blue litmus red showing that acid-forming precursors were liberated in the photolysis. Light sensitivity is required for applications as photoacid generators making these compounds potentially useful in the field. However, they must also be soluble in appropriate solvents used in the industry such as propylene glycol methyl ether acetate (PGMEA) or ethyl lactate. Although compound **13** is soluble in these solvents, compound **11** has poor solubility in them.

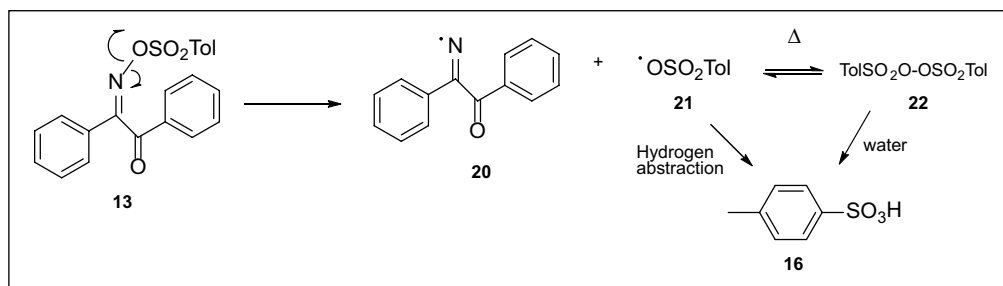


Figure 12. The proposed scheme for the fragmentation of oxime sulfonate **13** to release 4-methylbenzenesulfonic acid **16**.

Conclusion

The crystal structures of compounds **11–14** verify their oxime stereochemistry. Photochemical decomposition of the representative compounds **11** and **13** gave 4-methylbenzenesulfonic acid **16** which was observed in the ^1H and ^{13}C NMR spectra of the crude product in D_2O . Irradiation of both compounds **11** and **13** gave solutions in water that turned blue litmus paper red. This work provides evidence that the class of acid released from the irradiation of oxime sulfonates is a sulfonic acid, which might catalyse modification of a polymer resist during development.^{4,8,10,11} Irradiation of compound **11** did not give the expected 1,8-dicarbonitrile **18** and irradiation of compound **13** did not give benzonitrile **19** in easily detectable amounts. The efficient release of acid and good solubility suggest that compound **13** has potential use as a photoacid generator but acid is not liberated directly and requires a secondary hydrogen abstraction step or hydrolysis step.

Experimental

General: IR spectra were recorded on a diamond anvil spectrophotometer. UV spectra were recorded using a Perkin-Elmer Lambda 25 UV-Vis spectrometer with ethyl alcohol (EtOH) as the solvent. ^1H and ^{13}C NMR spectra were recorded at 600 and 150 MHz, respectively, using a Varian 400 spectrometer. Chemical shifts, δ , are given in ppm relative to the residual solvent and coupling constants, and J values are given in Hz. Low- and high-resolution mass spectra were obtained at the University of Wales, Swansea using electron impact ionisation and chemical ionisation. Melting point (m.p.) values were determined on a Kofler hot-stage microscope. Irradiations were done in a 100-mL immersion well with a Photochemical Reactors 6-W lamp (Reading, UK) and air cooling from a fume hood fan. No water flow was required with dichloromethane (DCM) as a solvent. Reflective foil was used to shield the lamp. The method is user friendly for students.

General procedure for di-oximes or mono-oximes

Acenaphthylene-1,2-dione di-oxime **9**

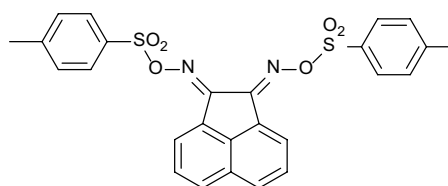
A literature procedure was followed but the work-up was different.¹⁵ Acenaphthenequinone (5.0 g, 27.5 mmol),

hydroxylamine hydrochloride (4.2 g, 60.4 mmol) and sodium acetate (5.0 g, 61 mmol) were stirred at room temperature (rt) in EtOH (150 mL) for 24 h. The mixture was gently refluxed for 2 h and then cooled. The mixture was poured into water (400 mL) and left to stand for 2 h as the product precipitated. This was filtered with a large sinter, washed with water (100 mL) and air dried to give the *title compound* (5.2 g, 98%) as an off-white solid, m.p. > 220 °C (from DCM/light petroleum ether 40–60). λ_{max} (EtOH)/nm 325 (log ϵ 3.2), 232 (4.6) and 212 (4.5); ν_{max} (Diamond) 3453w, 3018w, 2837w, 1489w, 1418w, 1347w, 1289w, 1228w, 1185w, 1146w, 1016m, 1000m, 937m, 854s, 825s, 773s, 611m, 539m and 443s; δ_{H} (600 MHz; CDCl_3) 7.69 (2H, m), 7.97 (2H, d, $J=6.0$) and 8.43 (2H, d, $J=6.0$); δ_{C} (150 MHz; CDCl_3) 125.5, 127.1, 127.8, 129.0, 130.6, 136.9 and 149.6; m/z (Orbitrap ASAP) 213.0659 ($\text{M}^+ + \text{H}$, 100%) $\text{C}_{12}\text{H}_9\text{N}_2\text{O}_2$ requires 213.0659.

Benzil-1,2-dione mono-oxime **10**

This was made by the same method.¹⁶

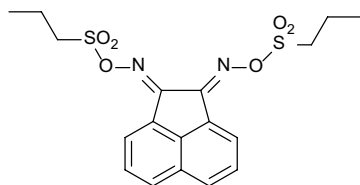
Synthesis of di-oxime and oxime sulfonates



(1E,2E)-Acenaphthylene-1,2-dione-O,O-ditosyl di-oxime **11**

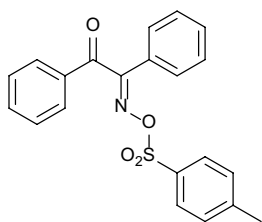
The bis-oxime of acenaphthenequinone **11** (400 mg, 1.9 mmol), 4-methylbenzenesulfonyl chloride (863 mg, 4.5 mmol) and Et_3N (457 mg, 4.5 mmol) were stirred in CH_2Cl_2 (100 mL) for 24 h at rt. The clear organic layer was washed with water (100 mL \times 2) and dried over MgSO_4 . The solution was concentrated under reduced pressure to a solid and then extracted three times by swirling with light petroleum ether (100 mL) which removed excess 4-methylbenzenesulfonyl chloride. Swirling with a smaller amount of DCM (30 mL) removed brown impurities and gave a product (470 mg, 48%). Proton NMR analysis showed this product to be impure, containing triethylammonium

tosylate, so it was dissolved in DCM (300 mL) and extracted with water (100 mL \times 3) and concentrated under reduced pressure to give the *title compound* (0.34 g, 35%) as a pale yellow solid, m.p. $> 220^\circ\text{C}$ (from DCM/light petroleum ether 40–60). λ_{max} (EtOH)/nm 333 (log ϵ 3.3), 316 (3.3), 245–280sh (3.5) and 229 (4.2); ν_{max} (Diamond) 1596w, 1575w, 1490w, 1390w, 1368w, 1178s, 1093m, 816s, 773s, 685s, 661s, 615s and 458m; δ_{H} (600 MHz; CDCl_3) 2.42 (6H, s), 7.31 (4H, d, $J=12.0$), 7.62 (2H, t, $J=6.0$ and 6.0), 7.92–7.95 (6H, m) and 8.33 (2H, d, $J=6.0$); δ_{C} (150 MHz; CDCl_3) 21.7, 126.7, 128.4, 128.8, 129.5, 129.7, 130.1, 130.5, 131.8, 138.8, 145.7, 155.2; m/z (Orbitrap ASAP) 521.0842 ($\text{M}^+ + \text{H}$, 100%) $\text{C}_{26}\text{H}_{21}\text{N}_2\text{O}_6\text{S}_2$ requires 521.0841; 179.0603 (naphthalene-1,8-dicarbonitrile + H, 50%) $\text{C}_{12}\text{H}_7\text{N}_2$ requires 179.0609.



(1E,2E)-Acenaphthylene-1,2-dione-O,O-dipropylsulfonyl di-oxime **12**

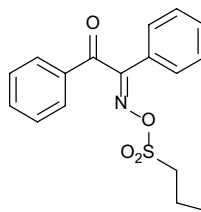
The bis-oxime of acenaphthenequinone **11** (1.0 g, 4.7 mmol), propanesulfonyl chloride (1.34 g, 9.4 mmol) and Et_3N (0.95 g, 9.4 mmol) were stirred in CH_2Cl_2 (100 mL) for 24 h at rt. The clear organic layer was washed with water (100 mL \times 2) and dried over MgSO_4 . The solution was concentrated under reduced pressure to a solid and then extracted by swirling with light petroleum ether (30 mL \times 10). Then concentration under reduced pressure gave the *title compound* (0.62 g, 31%) as a pale yellow solid, m.p. 215°C – 216°C (from DCM/light petroleum ether 40–60). λ_{max} (EtOH)/nm 331 (log ϵ 4.0), 316 (4.1) and 229 (4.9); ν_{max} (Diamond) 1687s, 1454w, 1365s, 1227m, 1173s, 948w, 811s, 732s, 683s, 629s, 580s, 539s and 497s; δ_{H} (600 MHz; CDCl_3) 1.17 (6H, t, $J=6.0$), 2.04 (4H, h, $J=6.0$), 3.58 (4H, t, $J=6.0$), 7.77 (2H, t, $J=6.0$), 8.11 (2H, d, $J=12.0$) and 8.49 (2H, d, $J=6.0$); δ_{C} (150 MHz; CD_3OD) 12.8, 17.3, 51.2, 126.7, 128.8, 128.9, 130.5, 130.6, 138.9, 156.0; m/z (Orbitrap ASAP) 425.0840 ($\text{M}^+ + \text{H}$, 100%) $\text{C}_{18}\text{H}_{21}\text{N}_2\text{O}_6\text{S}_2$ requires 425.0840; 179.0606 (naphthalene-1,8-dicarbonitrile + H, 95%) $\text{C}_{12}\text{H}_7\text{N}_2$ requires 179.0609.



(E)-1,2-Diphenyl-2-[(tosyloxy)imino]ethan-1-one **13**

The mono-oxime of benzil **12** (2.0 g, 8.9 mmol),¹⁵ 4-methylbenzenesulfonyl chloride (3.4 g, 17.8 mmol) and Et_3N

(2.1 g, 21.0 mmol) were stirred in CH_2Cl_2 (100 mL) for 24 h at rt.¹⁶ The clear organic layer was washed with water (100 mL \times 2) and dried over MgSO_4 . The solution was concentrated under reduced pressure to an oil which was swirled with light petroleum ether (30 mL \times 3) and left to crystallise. The solid was then extracted by swirling with light petroleum ether (30 mL \times 7) and concentrated under reduced pressure. The solid was then dissolved in DCM (100 mL) and filtered through a pad of silica to give the *title compound* (1.8 g, 53%) as a pale yellow solid, m.p. 121°C – 122°C (from DCM/light petroleum ether 40–60) on evaporation of the solvent. λ_{max} (EtOH)/nm 256 (log ϵ 4.3), 232 (4.2) and 207 (4.6); ν_{max} (Diamond) 1680s, 1594w, 1446w, 1371s, 1230m, 1174s, 1091w, 759s, 719s, 660s, 579s, 545s, 515s and 470m; δ_{H} (600 MHz; CDCl_3) 2.38 (s, 3H), 7.37 (4H, m), 7.48 (3H, m), 7.57 (2H, d, $J=6.0$), 7.66 (1H, t, $J=6.0$ and 12.0) and 7.85 (4H, t, $J=6.0$ and 6.0); δ_{C} (150 MHz; CDCl_3) 21.8, 127.5, 128.9, 129.0, 129.2, 129.3, 129.5, 129.8, 132.2, 132.3, 133.7, 135.2, 145.5, 163.2 and 190.1; m/z (EI) 397.1211 ($\text{M}^+ + \text{NH}_4$, 100%) $\text{C}_{21}\text{H}_{21}\text{N}_2\text{O}_4\text{S}$ requires 397.1217 (Orbitrap ASAP); 104.0519 (benzonitrile + H, 100%) $\text{C}_7\text{H}_6\text{N}$ requires 104.0500.



(E)-1,2-Diphenyl-2-[(propylsulfonyl)oxy]imino]ethan-1-one **14**

The mono-oxime of benzil **12** (1.0 g, 4.2 mmol), propanesulfonyl chloride (1.0 mL, 8.4 mmol) and Et_3N (0.85 g, 8.4 mmol) were stirred in CH_2Cl_2 (100 mL) for 24 h at rt. The clear organic layer was washed with water (100 mL \times 2) and dried over MgSO_4 . The solution was concentrated under reduced pressure to a solid and then extracted by swirling with light petroleum ether (30 mL \times 10). This gave the *title compound* (1.3 g, 89%) as a colourless solid, m.p. 126°C – 127°C (from DCM/light petroleum ether 40–60). λ_{max} (EtOH)/nm 255 (log ϵ 3.7) and 208 (4.1); ν_{max} (Diamond) 1680s, 1379m, 1367m, 1172s, 841m, 829m, 806s, 796s, 773s, 568s, 519m, 519m and 493m; δ_{H} (600 MHz; CDCl_3) 1.09 (3H, t, $J=6.0$ and 6.0), 1.92 (2H, m), 3.37 (2H, t, $J=6.0$ and 8.0), 7.45 (2H, t, $J=6.0$ and 12.0), 7.54 (3H, t, $J=6.0$ and 12.0), 7.66–7.73 (3H, m) and 7.97 (2H, d, $J=12.0$); δ_{C} (150 MHz; CDCl_3) 12.8, 17.1, 51.2, 127.7, 128.8, 129.3, 129.4, 129.6, 132.5, 133.6, 135.4, 163.9 and 190.0; m/z (Orbitrap ASAP) 349.1215 ($\text{M}^+ + \text{NH}_4$, 20%). $\text{C}_{17}\text{H}_{21}\text{N}_2\text{O}_4\text{S}$ requires 349.1222.

Photochemical irradiations

In total, 200 mg of compounds **11** or **13** were irradiated with a 6-W lamp for 5 h in 100 mL of CH_2Cl_2 without deoxygenation. The solution was concentrated and TLC analysis showed that extensive decomposition of the starting

material had occurred. The crude products were both shown to contain 4-methylbenzenesulfonic acid **16** by ^1H NMR. δ_{H} (400 MHz; D_2O) 2.20 (3H, s), 7.11 (2H, d, $J=8.0$) and 7.45 (2H, d, $J=8.0$); δ_{C} (150 MHz; D_2O) 20.4, 125.2, 129.3, 139.3 and 142.3. From the irradiation of compound **11**, ν_{max} (diamond anvil) 1678 cm^{-1} ; from the irradiation of compound **13**, ν_{max} (diamond anvil) 1682 cm^{-1} . Standard of 4-methylbenzenesulfonic acid **16** δ_{H} (400 MHz; D_2O) 2.10 (3H, s), 7.00 (2H, d, $J=8.0$) and 7.41 (2H, d, $J=8.0$); δ_{C} (150 MHz; D_2O) 20.4, 125.2, 129.3, 139.3 and 142.3; standard of 4-methylbenzenesulfonic acid **17** δ_{H} (400 MHz; D_2O) 2.29 (3H, s), 7.27 (2H, d, $J=8.0$) and 7.46 (2H, d, $J=8.0$); δ_{C} (150 MHz; D_2O) 20.6, 123.5, 129.6, 141.1 and 150.5.

Crystal structure determinations

Single crystals of **11–14** were recrystallised from DCM/light petroleum ether solution. Intensity data for **11–14** were collected at $T=100\text{ K}$ using a Rigaku AFC11 charge-coupled device (CCD) diffractometer (Mo $K\alpha$ radiation, $\lambda=0.71073\text{ \AA}$ for **11** and **13** and Cu $K\alpha$ radiation, $\lambda=1.54184\text{ \AA}$ for **12** and **14**). Each structure was easily solved by direct methods and the structural models were completed and optimised by least-squares refinement against $|F|^2$ using SHELXL-2014.²⁵ The crystal quality for **14** was notably poorer than for the other structures. For all structures, the H atoms were geometrically placed ($\text{C–H}=0.95\text{–}0.98\text{ \AA}$) and refined as riding atoms. The methyl groups were allowed to rotate, but not to tip, to best fit the electron density. The constraint $U_{\text{iso}}(\text{H})=1.2U_{\text{eq}}(\text{C})$ or $1.5U_{\text{eq}}(\text{methyl C})$ was applied in all cases.

11: $\text{C}_{26}\text{H}_{20}\text{N}_2\text{O}_6\text{S}_2$, $M_r=520.56$, pale orange column, $0.23 \times 0.06 \times 0.05\text{ mm}^3$, triclinic, space group $P\bar{1}$ (No. 2), $Z=2$, $a=7.9131(2)\text{ \AA}$, $b=11.5800(3)\text{ \AA}$, $c=14.4677(3)\text{ \AA}$, $\alpha=103.676(2)^\circ$, $\beta=95.088(2)^\circ$, $\gamma=109.671(2)^\circ$, $V=1192.28(5)\text{ \AA}^3$ at 100 K . Number of measured and unique reflections=20,472 and 5452, respectively ($-10 \leq h \leq 10$, $-15 \leq k \leq 15$, $-18 \leq l \leq 18$; $2\theta_{\text{max}}=50.5^\circ$; $R_{\text{int}}=0.017$). Final $R(F)=0.035$, $wR(F^2)=0.093$ for 327 parameters and 4971 reflections with $I > 2\sigma(I)$ (corresponding R -values based on all 5452 reflections=0.039 and 0.095, respectively), Cambridge Crystallographic Data Centre (CCDC) deposition number 1870464.

12: $\text{C}_{18}\text{H}_{20}\text{N}_2\text{O}_6\text{S}_2$, $M_r=424.48$, pale yellow block, $0.23 \times 0.21 \times 0.18\text{ mm}^3$, triclinic, space group $P\bar{1}$ (No. 2), $Z=4$, $a=7.06267(6)\text{ \AA}$, $b=11.08547(10)\text{ \AA}$, $c=25.1261(2)\text{ \AA}$, $\alpha=96.2327(6)^\circ$, $\beta=90.5797(8)^\circ$, $\gamma=95.8034(7)^\circ$, $V=1945.10(3)\text{ \AA}^3$ at 100 K . Number of measured and unique reflections=34,798 and 7043, respectively ($-8 \leq h \leq 8$, $-13 \leq k \leq 13$, $-30 \leq l \leq 30$; $2\theta_{\text{max}}=136.5^\circ$; $R_{\text{int}}=0.015$). Final $R(F)=0.029$, $wR(F^2)=0.082$ for 509 parameters and 6850 reflections with $I > 2\sigma(I)$ (corresponding R -values based on all 7043 reflections=0.030 and 0.082, respectively), CCDC deposition number 1870465.

13: $\text{C}_{21}\text{H}_{17}\text{NO}_4\text{S}$, $M_r=379.42$, colourless block, $0.27 \times 0.12 \times 0.04\text{ mm}^3$, monoclinic, space group Ia (No. 9), $Z=4$, $a=13.0319(6)\text{ \AA}$, $b=12.1421(5)\text{ \AA}$, $c=11.8439(5)\text{ \AA}$, $\beta=102.396(5)^\circ$, $V=1830.42(14)\text{ \AA}^3$ at 100 K . Number of measured and unique reflections=10,604 and 3801,

respectively ($-16 \leq h \leq 15$, $-15 \leq k \leq 15$, $-15 \leq l \leq 15$; $2\theta_{\text{max}}=55.0^\circ$; $R_{\text{int}}=0.035$). Final $R(F)=0.029$, $wR(F^2)=0.076$ for 245 parameters and 3610 reflections with $I > 2\sigma(I)$ (corresponding R -values based on all 3801 reflections=0.031 and 0.077, respectively), Flack absolute structure parameter=0.02 (4), CCDC deposition number 1870466.

14: $\text{C}_{17}\text{H}_{17}\text{NO}_4\text{S}$, $M_r=331.37$, colourless needle, $0.30 \times 0.03 \times 0.01\text{ mm}^3$, triclinic, space group $P\bar{1}$ (No. 2), $Z=2$, $a=5.2869(4)\text{ \AA}$, $b=9.1995(12)\text{ \AA}$, $c=16.829(2)\text{ \AA}$, $\alpha=97.497(11)^\circ$, $\beta=95.822(8)^\circ$, $\gamma=94.282(9)^\circ$, $V=804.11(16)\text{ \AA}^3$ at 100 K . Number of measured and unique reflections=10,351 and 2857, respectively ($-5 \leq h \leq 6$, $-10 \leq k \leq 10$, $-19 \leq l \leq 20$; $2\theta_{\text{max}}=135.0^\circ$; $R_{\text{int}}=0.129$). Final $R(F)=0.119$, $wR(F^2)=0.307$ for 209 parameters and 1982 reflections with $I > 2\sigma(I)$ (corresponding R -values based on all 2857 reflections=0.158 and 0.338, respectively), CCDC deposition number 1870467.

Acknowledgements

We are grateful to the National Mass Spectrometry Foundation, University of Swansea and to the National Crystallographic Service Centre, University of Southampton.

Declaration of conflicting interests

The author(s) declared no potential conflicts of interest with respect to the research, authorship and/or publication of this article.

Funding

The author(s) received no financial support for the research, authorship and/or publication of this article.

Supplemental material

CCDC deposition numbers 1870464–1870467 contain the supplemental crystallographic data for this paper. These data can be obtained free of charge from the Cambridge Crystallographic Data Centre at www.ccdc.cam.ac.uk/data_request/cif

References

1. Ito H. *Adv Polym Sci* 2005; 172: 37.
2. Moore's Law, https://en.wikipedia.org/wiki/Moore%27s_law (December 2018).
3. Robinson APG and Lawson RA. *Materials and processes for next generation lithography* (Frontiers of Nanoscience, vol. 11) (ed. RE Palmer). Amsterdam: Elsevier, 2016.
4. Asakura T, Yamoto H, Ohwa M, et al. US6512020 B1, 28 March 2001, Ciba Speciality Chemicals Corporation.
5. Crivello JV and Lam JHW. *Macromolecules* 1977; 10: 1307.
6. Crivello JV and Lam JHW. *J Poly Sci* 1979; 17: 977.
7. Crivello JV and Reichmanis E. *Chem Mat* 2014; 26: 533.
8. Dietliker K, Rutsch W, Berner G, et al. US4736055, 11 April 1986, Ciba-Geigy Corporation.
9. Cho YJ, Ouyang CY, Krysak M, et al. *P SPIE Adv Resist Mat Proc Tech* 2011; 7972.
10. Schroer H, Goliasch K and Beck U. US4233233, 11 November 1980, Bayer Aktiengesellschaft.
11. Dietliker K, Kunz M, Yamato H, et al. US0013974 A1, 22 January 2004, Ciba Speciality Chemicals Corporation.

12. Li L, Liu X, Pal S, et al. *Chem Soc Rev* 2017; 46: 4855.
13. Reichmanis E, Nalamasu O and Houlihan FM. *Acc Chem Res* 1999; 32: 659.
14. Nandi S, Yogesh M, Reddy PG, et al. *Mat Chem Front* 2017; 1: 1895.
15. Crosby J, Rennie RAC, Tanner J, et al. US4014893, 28 March 1977, Imperial Chemical Industries Limited.
16. Danilewicz JC. *J Chem Soc (C)* 1970; 1049.
17. Pilgram K. *J Org Chem* 1970; 35: 1165.
18. Richtar J, Heinrichova P, Apaydin DH, et al. *Molecules* 2018; 23: 2271.
19. Essa AH, Al-Shamkhani ZAN, Jalbout AF, et al. *Heterocycles* 2008; 75: 2235.
20. Warad I, Ghazzali M, Al-Resayes S, et al. *Zeit Krist NCS* 2010; 225: 611.
21. Dvorak T, Rečnik L-M, Schnürch M, et al. *ARKIVOC* 2013; iii: 245.
22. Nieger M, Schallenberg A and Wamhoff H. CSD Communication (deposition number 227981), 2004.
23. Fier PS. *J Amer Chem Soc* 2017; 139: 9499.
24. Jones PG, Edwards MR and Kirby AJ. *Acta Cryst* 1986; C42: 1228.
25. Sheldrick GM. *Acta Cryst* 2015; C71: 3.